IEEE Access
Multidisciplinary | Rapid Review | Open Access Journal

Received February 25, 2020, accepted March 4, 2020, date of publication March 9, 2020, date of current version March 18, 2020.

Digital Object Identifier 10.1109/ACCESS.2020.2979256

Arrhythmia Recognition and Classification Using Combined Parametric and Visual Pattern Features of ECG Morphology

HUI YANG[1,2], (Member, IEEE), AND ZHIQIANG WEI[2]
[1]Department of Computer Foundation, Ocean University of China, Qingdao 266100, China
[2]College of Information Science and Engineering, Ocean University of China, Qingdao 266100, China

Corresponding authors: Hui Yang (yanghuiouc@163.com) and Zhiqiang Wei (zhiqiangweiouc@126.com)

This work was supported in part by the Humanities and Social Sciences Project of Chinese Ministry of Education under Grant 17YJC880116, in part by the National Natural Science Foundation of China under Grant 61672475, and in part by the Marine S&T Fund of Shandong Province for Pilot National Laboratory for Marine Science and Technology (Qingdao) under Grant 2018SDKJ0402.

ABSTRACT ECG is a non-invasive tool used to detect cardiac arrhythmias. Many arrhythmias classification solutions with various ECG features have been reported in literature. In this work, a new method combined with a novel morphological feature is proposed for accurate recognition and classification of arrhythmias. First, the events of the ECG signals are detected. Then, parametric features of ECG morphology, i.e., amplitude, interval and duration, are extracted from selected ECG regions. Next, a novel feature for analyzing QRS complex morphology changes as visual patterns as well as a new clustering-based feature extraction algorithm is proposed. Finally, the feature vectors are applied to three well-known classifiers (neural network, SVM, and KNN) for automatic diagnosis. The proposed method was assessed with all fifteen types of heartbeats as recommended by the Association for Advancement of Medical Instrumentation from the MIT-BIH arrhythmia database and achieved the best overall accuracy of 97.70% based on KNN, using the combined parametric and visual pattern features of ECG Morphology. The accuracies for the six main types – normal (N), left bundled branch blocks (L), right bundled branch blocks (R), premature ventricular contractions (V), atrial premature beats (A) and paced beats (P) are 97.79%, 99.50%, 99.59%, 97.69%, 89.70%, and 99.92%, respectively. Comparisons with peer works prove a marginal progress in automatic heart arrhythmia classification performance.

INDEX TERMS Classification, ECG morphology, feature extraction.

I. INTRODUCTION

Cardiovascular disease (CVD) has become one of the leading causes of non-infectious and non-transmissible disease deaths in the world [1]. Many cardiac arrests and sudden deaths are attributed to the cardiac arrhythmias [2]. Cardiac arrhythmias, also called cardiac dysrhythmias, are caused by alterations in the formation and conduction of electrical impulses through the myocardial tissue, which may modify the origin and physiological diffusion of the electrical stimulus of the heart and can vary in severity from entirely benign to arrhythmias with an immediate risk of life [2].

Electrocardiogram (ECG) is the most widely disseminated and easy-to-apply method to measure the cardiac activity of a patient. Every heartbeat cycle consists of the successive atrial depolarization and ventricular depolarization [3]. This cardiac activity begins at the atrial sine node and propagates though the rest of the heart, resulting in electrical currents on the surface of the body and provoking variations in the electrical potential of the skin surface. These signals can be measured by adding surface electrodes to patient's body and then graphically represented in the ECG record.

The main features of a single normal cycle of the ECG, are traditionally reflected by the amplitudes, morphologies, durations of individual waves (P, Q, R, S, T, and U), intervals (PP, PR, RR, ST and QT), and segments (PR and ST) [4] as shown in Fig. 1. The QRS complex is the most significant wave in the ECG signal. Due to some blocked regions in the ventricles, existence of ectopic center, and heartbeats provoked by pacemaker, the path of propagation through the

The associate editor coordinating the review of this manuscript and approving it for publication was Derek Abbott.

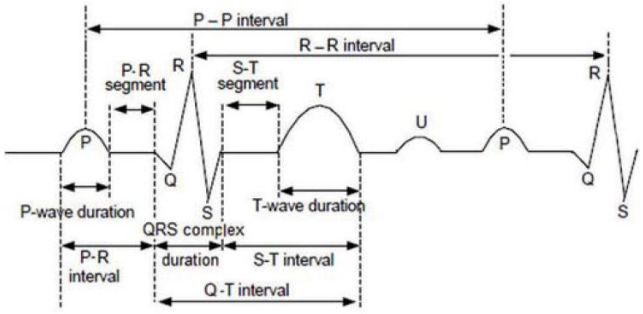

FIGURE 1. A general structure of an ECG signal waveform.

ventricles could be changed and cause irregular waveforms of QRS complex. Hence, medical practitioners can detect various types of cardiac arrhythmia, such as, left bundled branch blocks (L), right bundled branch blocks (R), premature ventricular contractions (V), atrial premature beats (A), and paced beats (P), through the irregular changes in ECG waveforms.

As manual heartbeat classification of long-term ECG recordings is very time-consuming and needs a lot of practice for junior doctors, automatic recognition and classification system is a high-efficient way for diagnosis and could ultimately improve the quality of treatment.

A. RELATED WORKS

A full ECG arrhythmia recognition and classification system can be divided into three main parts, as follows: 1) preprocessing, 2) feature extraction, and 3) heartbeat classification.

In order to remove baseline wander, electromyographic (EMG) noise, and power line interference contained in the ECG signal, numerous methods have been proposed, such as bandpass filters [5], wavelet transform based methods [6], [7], adaptive filters [8], empirical mode decomposition [9], and independent component analysis [10]. For example, Rakshit and Das [9] have proposed a methodology using EMD which decomposes signals as a set of intrinsic mode function (IMF) based on the signal complexity for removing noise interference. Jung and Lee [7] have employed Daubechies 4 as the wavelet basis function to remove the noise within the ECG signal in the preprocessing stage.

Afterwards, appropriate features can be calculated from specific parts of the preprocessed signal based on various techniques in feature extraction stage.

In the classification stage, the feature vectors are grouped to train some types of classifiers. Based on a comprehensive literature survey, there is an abundance of ECG classification algorithms having been employed up to now, such as neural network (NN) [11], SVM [11], [12], decision tree [13], logistic regression [14], linear discriminant [15], neuro-fuzzy system [16], K-nearest neighbors (KNN) classification method [17], [18], etc., among which neural networks (NN), support vector machines (SVM), and K-Nearest Neighbors (KNN) are extensively used algorithms in literature for this task. For example, in [18], the KNN classifier feeding genetic algorithm features achieved a higher accuracy of 99.30% than SVM and NN for categorizing 6318 samples of ECG beats into nine types.

This work mainly focuses on the feature extraction stage, which is the key to the success in automatic cardiac arrhythmia recognition and classification using the ECG signals. Any hidden information extracted from the ECG signals used to discriminate arrhythmia types could be considered as a feature. Several feature extraction methods have been proposed in literature for analysis of ECG signals, and these methods can be grouped into two main types, which are time domain and frequency domain.

In the time domain, the simplest way to extract features is to utilize the points of the segmented ECG curve, i.e., the heartbeat, as features [19]. However, the main drawback of this method is that it is not very efficient since it produces a high dimension feature vector. In addition, it might suffer from scale or displacement of the signal with respect to the fiducial point R [20]. As a result, a classification accuracy of 85% was reported in [19]. The most common feature reported in literature is the inter-beat R wave interval, which is the time between the successive R waves, namely, RR interval [21]. For example, Lin and Yang [21] have confirmed the use of a normalized RR interval improves the classification results. Other RR-based features, such as pre-RR, post-RR, local-RR, and average-RR are also reported in [7], [8], [20], [22]. The RR intervals can also be measured for the construction of heart rate variability (HRV) signal, which is a more robust method since the RR intervals are less affected by the noise [9], [10], [23], [24]. Venkatesan *et al.* [25] have reported that using of HRV parameters, such as RR mean, RR standard deviation, RR triangular index, etc. could classify heartbeats into normal and abnormal classes in an abnormality detection system based on SVM classifier with a maximum accuracy of 96.00%.

Features correlated with the variations in the morphology of the ECG signal, such as parameters about amplitudes (P wave, R wave), intervals (PP, PR, ST and QT), durations (QRS complex, P wave, T wave), slopes, areas and curve length of QRS complex, are also widely used in literature. Among these morphological features, amplitudes, intervals and durations have been clinically studied [11], [19], [26]–[29]. Zhang *et al.* [29] have adopted ECG features, including inter-beat and intra-beat intervals, amplitude, area, and morphological distance in heartbeat classification with an average accuracy of 86.66% and confirmed the discrimination power of RR interval, P wave morphology and QRS complex morphology.

In frequency domain, the discrete wavelet transform (DWT) is the most widely used method [30]–[33]. Some researchers have identified DWT as the best method for extracting features from ECG signal due to its advantage in multi-resolution analysis [30]–[33]. Various statistical features can be extracted from coefficients of DWT, such as, mean, standard deviation, energy and coefficient variance [33], [34]. In addition, other signal processing methods,

such as power spectral density (PSD), and high-order spectral (HOS), hexadecimal local pattern (HLP), structural co-occurrence matrix (SCM), have also been combined for extracting features of ECG signals [11], [32], [35]–[37]. The independent component analysis (ICA), principle component analysis (PCA) and genetic algorithm (GA) methods were used for dimensionality reduction [17], [38]–[41].

For example, Chawla [39] has proposed that ICA is more suitable for extracting features from ECG signals than PCA, because the ICA technique can separate individual sources from a mixing signal. Kar and Okandan [35] have shown that using average PSD of six-level decomposed ECG signals could improve the final classification results. Martis *et al.* [37] have reported to extract bispectrum features using HOS technique for identification of five types of heartbeats with an average accuracy of 93.48%. Tuncer *et al.* [32] have shown that using HLP technique to extract 512 dimensional features from each low pass filter of a five-level of DWT composition of 1000 randomly selected ECG signal fragments and obtained an accuracy of 95%. Marinho *et al.* [11] have proposed to apply SCM as a novel feature extraction technique in arrhythmia classification and achieved an accuracy 90.9% with SVM.

Besides, deep learning approach has also been employed for feature extraction of ECG signals [42]–[45]. In [42], Yang *et al.* have performed a feature extraction using DL-CCANet without any prior definition of which features should be used and obtained a 95.20% overall accuracy. Qian *et al.* [44] have constructed a 17-layer-deep convolutional neural network (CNN) using a genetic algorithm for classification of 5 ectopic heartbeat types with an accuracy of 95.78%. However, it is well known that when using a deep learning approach, it may not be easy to interpret the result and the computational cost is much higher than other methods. Additionally, numerous factors, such as, the number of hidden layers, the right number of neurons to use in the hidden layers, activation function, optimizer, strategy for preventing overfitting, etc., are required to be optimized in the neural network approach.

To sum up, although many existed features have shown their advantages in the field of arrhythmia discrimination and are correlated with mathematical computations, few of them are related to diagnostic standards or have physiological meaning which allows physicians to comprehend in an intuitive way. Whereas, existed clinical relevant features, such as amplitudes, durations, intra-beat and inter-beat intervals of character waves, have their own limitations. For example, the capacity to discriminate various types of the heartbeats using only the RR-based features is very limited. Some of the common arrhythmia types such as the left bundle branch block and the right bundle branch block beats could not be detected [23], [25]. The main drawback of simple parametric features of ECG morphology, such as amplitude, interval and duration, is the fact that they are not sufficient for describing the heartbeat morphology alternations in detail and the subtle changes in the amplitude, interval, and duration in the ECG do not provide good discrimination [46]. Therefore, it is still essential to further explore this field.

Inspired by the common knowledge to physicians that patients with the same disease have similar-looking ECG shape in the relevant channels and the fact that it is physicians' routine to make diagnosis through visual analysis of the ECG waveform in clinical practice, we propose a novel morphological feature based on visual pattern to represent the character of ECG heartbeats.

The contributions of this work are in the following aspects: 1) a novel ECG morphological feature, i.e., visual morphological pattern of QRS complex, is proposed to capture the fundamental intuition used by physicians; 2) a novel computational algorithm is proposed for feature extraction with advantage of low complexity; 3) the interpretability and discrimination capability of the arrhythmia recognition and classification system are improved; 4) a broad range of data and several frequently used classifiers were involved in evaluation; 5) the capability of classifying 15 heartbeat types; 6) a high performance and reliable system for heart arrhythmia classification with low cost and physiological meaning.

II. METHODS

The proposed arrhythmia recognition and classification system consists of three stages: preprocessing and detection, feature extraction, and heartbeat classification. The block diagram of the proposed heartbeat classification algorithm is shown in Fig. 2.

A. PREPROCESSING AND DETECTION

For preprocessing and heartbeat detection, Pan-Tompkins algorithm [47] is used in this stage. There are five steps in the algorithm: band-pass filtering, differentiation, squaring, moving window integration, and thresholds adjustment. A band pass filter constructed by the low pass and high pass filters is used to reduce noise, such as 60 Hz power line interference, muscle noise, and baseline wander from the raw ECG signals. And then, the signal is passed through a derivative operator to highlight the high slopes which distinguish the QRS complexes from other ECG waves. The next step is to square the signal point by point, so that the higher values which mainly present due to QRS complex are emphasized. The following integrating moving window sums the area under the squared waveform over a suitable interval and extracts the QRS onset, QRS offset and QRS width. Finally, the threshold adjust is applied to detect R peaks.

The detected QRS complex can be considered as a reference to detect P waves. Since the P wave duration is within the range of 0.11 ± 0.02 seconds [48], the P wave can be identified in a search window from QRS onset forwardly to 0.20 seconds (72 samples). The local distance transform method is adopted to locate the onset and offset of the P wave. P wave peak is located as the center of average integral.

B. FEATURE EXTRACTION

The feature extraction stage is crucial for the arrhythmia recognition and classification system. In practice, clinical

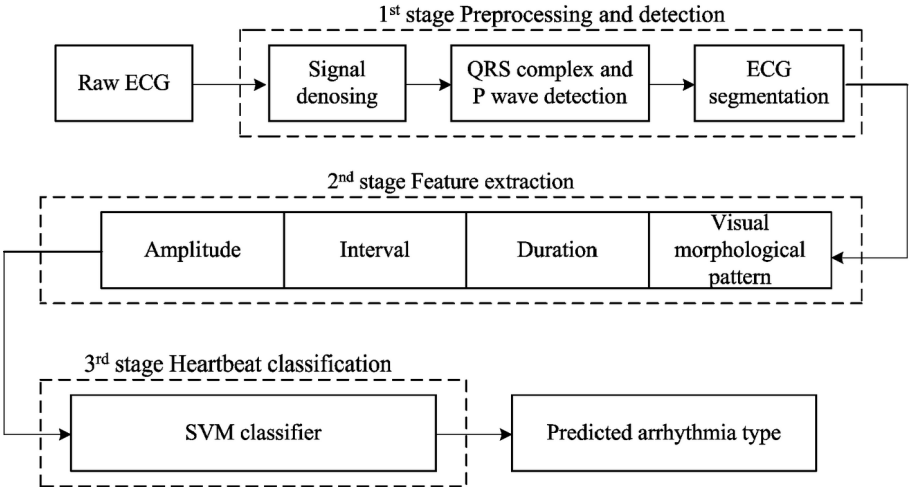

FIGURE 2. Proposed arrhythmia recognition and classification system.

experts are concerned about changes in waveforms, through which they can interpret various cardiac dysfunctions [28]. However, many information is not evident in the ECG signal. Hence, the feature extraction in our study aims to extract those diagnostic standards related characteristics of the ECG morphology to increase the interpretability and reliability of the diagnosis algorithm.

In this work, a total of eight features representing amplitude, interval, duration and a new introduced feature, visual pattern of the QRS complex, are extracted for classification of 15 types of atrial and ventricular arrhythmias in [49].

1) PARAMETRIC FEATURE BASED ON THE ECG MORPHOLOGY

Since atrial depolarization corresponds to P wave and ventricular depolarization corresponds to QRS complex, seven parametric features are calculated, as shown in Fig. 1.

The P wave morphology can reveal right or left atrial hypertrophy or atrial arrhythmias. A normal P wave should be upright, with a maximal amplitude less than 0.12 mV in amplitude and a duration shorter than 0.12 seconds [48]. Hence, amplitude of P wave and P wave duration are selected in this work. In addition, PP interval and PR interval are also included in the feature vector. PP interval represents the interval between the P waves due to atrial depolarization. PR interval extends from the beginning of the P wave (the onset of atrial depolarization) until the beginning of the QRS complex (the onset of ventricular depolarization), reflecting how fast the impulse travels from the atriums through the atrioventricular valve to the ventricles. The PR interval is also termed as PQ interval. A normal PR (PQ) interval is within a range of 0.16 ± 0.04 seconds [48].

Besides, as important characteristics of QRS complex, the amplitude of R wave, QRS duration, and RR interval are also taken into account because QRS complex is the main wave in ECG signal and represents the process of the ventricular depolarization. The QRS complex normally lasts 0.10 ± 0.02 seconds in width and is less than 2.00 mV in amplitude. RR interval refers to the time between the current R peak of a heartbeat and the next R peak in this work. A typical normal value of RR interval is within a range of 0.60 to 1.00 seconds.

2) VISUAL MORPHOLOGY PATTERN FEATURE BASED ON A PROPOSED ALGORITHM FOR CLUSTERING QRS COMPLEX MORPHOLOGY

The QRS complex, consisting of Q wave, R wave and S wave, is the most visually obvious graphical deflection seen on a typical ECG signal and the most utilized. A Q wave is any downward deflection immediately following the P wave. An R wave follows as an upward deflection, and the S wave is any downward deflection after the R wave. They correspond to the depolarization of the right and left ventricles of the human heart and contraction of the large ventricular muscles. However, the patterns provoked by arrhythmias can deeply alternate the waveform of QRS complex. It is common knowledge to physicians that the same atrial or ventricular arrhythmia has similar-looking ECG pattern. Some examples of such similarity can be seen from Fig. 3. Therefore, in practice, correct interpretation of difficult ECGs requires exact labeling of the various waves by human.

Considering morphology of the QRS complex is a significant discriminating feature stipulated for arrhythmia diagnosis in ECG-based clinical practice [20], [27], and the same arrhythmia shares similarity in ECG shapes, a novel feature, visual morphological pattern of QRS complex (VMP-QRS), as well as a new clustering-based feature extraction algorithm, named as adaptive K-means clustering (AKMC) algorithm, is proposed by authors of this work for analyzing QRS complex changes as a virtual image.

The proposed AKMC algorithm is based on the theory of the K-means clustering algorithm. K-means algorithm is

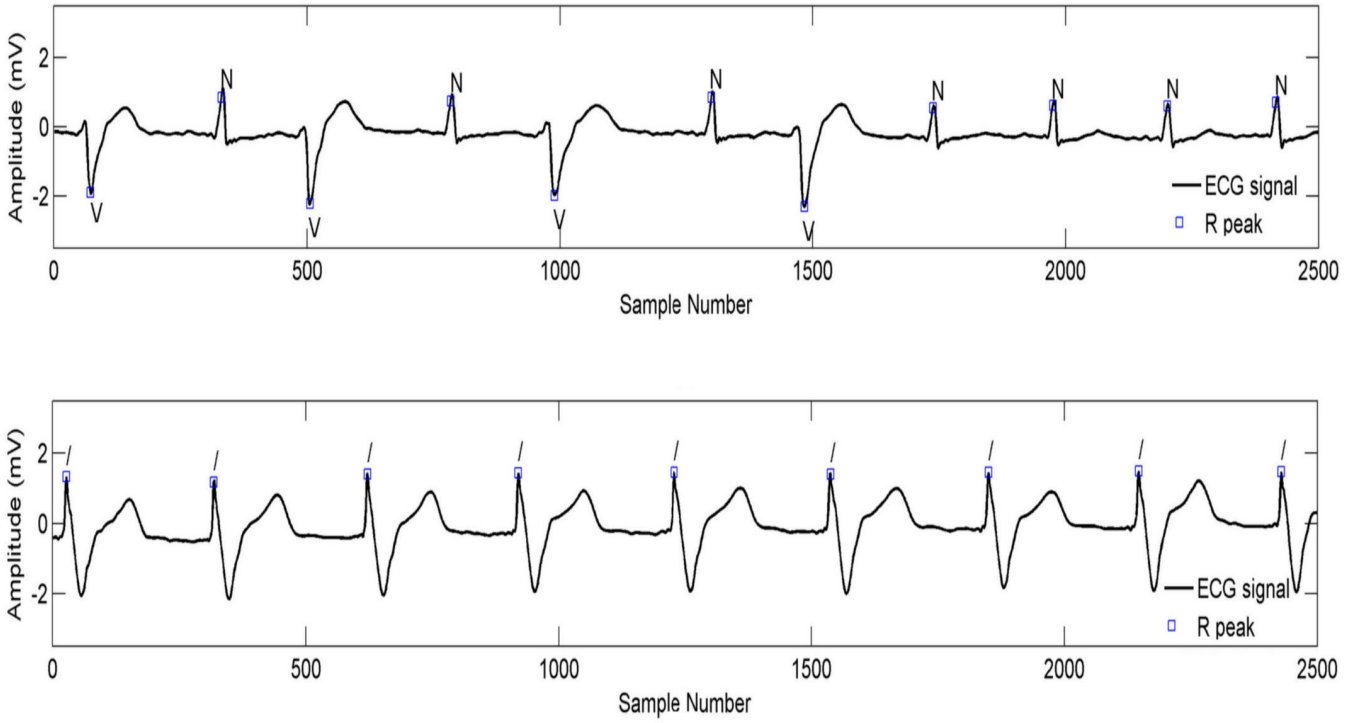

FIGURE 3. Illustration of similarity of ECG pattern for similar arrhythmia with type annotations on each R peak: 'N', 'V', and '/' denote normal beat, premature ventricular contraction beat, and paced beat, respectively.

a widely used method in cluster analysis. It classifies a set of vectors $\boldsymbol{X} = \{x_1, x_2, \ldots, x_N\}$ ($X \subset R^N$) into K different clusters $C_k (k = 1, \ldots, K)$ according to the Euclidean norm of $\boldsymbol{R}^N$ [50]. Each cluster is characterized by a centroid that is the barycenter of all the points in the cluster. The proposed AKMC algorithm adopts the idea of K-means algorithm to cluster QRS complex vectors with similarity in Euclidean distance so that the medical practitioners could understand and interpret the clustering result in an intuitive way. On the other hand, unlike the k-means clustering algorithm, which determines the number of clusters in the early stage and the number of clusters cannot change as long as the iteration is done, the proposed AKMC algorithm improves the K-means algorithm by allowing the number of the centroids to be changed based on the iteration process. In the meanwhile, only a small number of parameters are required in the proposed AKMC algorithm. The pseudocode of the proposed AKMC algorithm for VMP-QRS feature extraction is given in Algorithms 1. The detailed description of the AKMC algorithm for VMP-QRS extraction is listed as follows.

In the first step, the QRS complex is segmented from the ECG signal and standardized. Since the QRS duration is less than 0.12 seconds and the sampling rate of the most utilized MIT-BIH arrhythmia database [49] is 360 Hz, a window of 50 samples within the range of [R peak - 20, R peak + 29] are adopted as the segment vector. In order to reduce influence caused by the different magnitudes or variances, all samples used in this algorithm are Z-score standardized according to Equation (1) as below:

$$x(i) = \frac{s(i) - \frac{1}{L}\sum_{k=1}^{L} s(k)}{\sqrt{\frac{1}{L-1}\sum_{i=1}^{L}\left(s(i) - \frac{1}{L}\sum_{k=1}^{L} s(k)\right)^2}}, i = 1, 2, \cdots, L., \quad (1)$$

where $s(i)$ is the ith component of QRS complex vector s; $L = 50$ is the length of s. The data are represented as a collection of vectors $\boldsymbol{X} = \{x_1, x_2, \ldots, x_N\}$, where N is the number of vectors.

Suppose that $C_{\max}$, C, and n_k are the estimated total number of clusters, the actual created total number of clusters, and the number of QRS complex vectors assigned to the cluster δ_k, respectively.

In the second step, take the first QRS complex vector x_1 as the centroid of the first cluster δ_1 and set C to 1.

In the third step, calculate the Euclidean distance between each QRS complex vector x_i ($i \in \{1, 2, \ldots, N\}$) and centroid μ_j of each cluster δ_j ($j \in \{1, 2, \ldots, C\}$) according to (2):

$$d\left(x_i, \delta_j\right) = \left(\sum_{t=1}^{L}\left(x_i(t) - \mu_j(t)\right)^2\right)^{1/2}. \quad (2)$$

Obtain the distance vector $\boldsymbol{D}$(j) as (3):

$$\boldsymbol{D}(j) = \left\{d\left(x_i, \delta_j\right)\right\}, \; j = 1, 2, \ldots, C. \quad (3)$$

Find the nearest cluster δ_k at which $d(x_i, \delta_k)$ has a minimum in $\boldsymbol{D}(j)$, namely $d_{\min} = \min(\boldsymbol{D}(j)) = d(x_i, \delta_k)$. If $d_{\min}$ is less

Algorithm 1 The AKMC Algorithm for VMP-QRS Feature Extraction.

Input:
−Raw QRS complex segment vectors $S = \{s_1, s_2, \ldots, s_N\}$, where N is the number of vectors
−$C_{\max}$, the estimated total number of clusters
−T_c, the predefined clustering threshold
Output:
−The cluster label set of the QRS complex vectors

Perform Z-score standardization to the segment vectors using Equation (1) and represent the data as a collection of QRS complex vectors $X = \{x_1, x_2, \ldots, x_N\}$, where N is the number of vectors
Set $C = 1$ /* C is the actual created total number of clusters */
Set $\mu_1 = x_1$ /* μ_j is the centroid of cluster $\delta_j, j \in \{1, 2, \ldots, C\}$ */
Set $n_1 = 0$ /* n_k is the number of QRS complex vectors assigned to the cluster δ_k */
Do
  for each QRS complex vector x_i, $x_i \in X$, $i \in \{1, 2, \ldots, N\}$ **do**
    Calculate $d(x_i, \delta_j), j \in \{1, 2, \ldots, C\}$ using Equation (2) and obtain $D(j)$ as Equation (3)
    Find the nearest cluster δ_k where $d_{\min} = \min(D(j)) = d(x_i, \delta_k)$
    if $d_{\min} \leq T_c$ **then**
      Assign x_i to the nearest cluster δ_k
      Update $\mu_k = (n_k \mu_k + x_i)/(n_k + 1)$ as Equation (4)
      Set $n_k = n_k + 1$
    else
      if $C < C_{\max}$ or $\min\{d(\delta_i, \delta_j)\} = d(\delta_p, \delta_q) \geq d_{\min}$ **then**
        Set x_i as the centroid of a new cluster
        Update $C = C + 1$
        Set $n_C = 1$
      else
        Merge the two clusters δ_p, δ_q to δ_p according to Equation (5)
        Set x_i as the centroid of the cluster δ_q
        Update $n_q = 1$
      end
    end
  end
Loop Until the centroids no longer change
return the cluster label set of the QRS complex vectors

than a predefined clustering threshold T_c, assign the vector x_i to the cluster δ_k, update the centroid of the cluster δ_k as (4):

$$\mu_k = (n_k \mu_k + x_i) \big/ (n_k + 1), \tag{4}$$

and set $n_k = n_k + 1$. Then go back to the third step. Otherwise, go to the fourth step.

In the fourth step, if C is less than $C_{\max}$, go to the sixth step. Otherwise, go to the fifth step.

In the fifth step, calculate the Euclidean distance between any two different clusters $d(\delta_i, \delta_j)$, where $i, j \in \{1, 2, \ldots, C\}$ and $i \neq j$. If $d(\delta_p, \delta_q)$ has a minimum in $\{d(\delta_i, \delta_j)\}$ where i, $j \in \{1, 2, \ldots, C\}$, and $d(\delta_p, \delta_q)$ is equal or greater than $d_{\min}$, go to the sixth step directly. Otherwise, merge the two clusters δ_p, δ_q to δ_p, update the centroid of δ_p as (5):

$$\mu_p = \left(n_p \mu_p + n_q \mu_q\right) \big/ \left(n_p + n_q\right), \; n_p = n_p + n_q \tag{5}$$

Set x_i as the centroid of the cluster δ_q, update $n_q = 1$ and then go back to the third step.

In the sixth step, set x_i as the centroid of a new cluster. Update $C = C + 1$ and set $n_C = 1$.

In the seventh step, repeat the third step until the centroids no longer change.

When the clustering process comes to an end, the cluster label $\delta_i (i = 1, 2, \ldots, C)$ which each QRS complex vector x_i belongs to is added as the VMP-QRS feature to the feature vector.

C. HEARTBEAT CLASSIFICATION

After the feature extraction stage, three different classifiers are applied here for assessment of arrhythmia classification.

1) NEURAL NETWORK

A neural network is a computational system consisting of interconnected group of nodes. In this work, the multiple feed-forward neural network (MLP) was employed. The goal of a MLP is to approximate some function $\boldsymbol{Y}$. For example, for a classifier, the output vector at iteration k can be expressed as (6):

$$\boldsymbol{Y}_k = f(\boldsymbol{X}, \boldsymbol{W}_k), \tag{6}$$

where $\boldsymbol{X}$ is the input vector and $\boldsymbol{Y}_k$ is the category mapped from input $\boldsymbol{X}$, $\boldsymbol{W}_k$ are the network weights which are modified as (7):

$$\boldsymbol{W}_{k+1} = \boldsymbol{W}_k - \left[\boldsymbol{J}^T\boldsymbol{J} + \mu\boldsymbol{I}\right]^{-1}\boldsymbol{J}^T\boldsymbol{e}, \tag{7}$$

where $\boldsymbol{J}$ is the Jacobian matrix with first derivatives of the network errors $\boldsymbol{e}$ with respect to the weights and μ is a dynamic parameter [51]. A classifier possessing one input layer, one hidden layer with 28 hidden layer neurons were chosen by trial and error for this task. The MLP training session are terminated after 200 iterations.

2) RADIAL BASIS FUNCTION BASED SUPPORT VECTOR MACHINE (RBF-SVM)

SVM [52] is a popular supervised learning method that is widely employed in pattern recognition, object identification, image processing and classification [53].

As a classifier, SVM converts the input vector to higher dimension space through some nonlinear mapping and obtains an optimal separating hyperplane, which minimizes the empirical classification error and maximizes the geometric margin. The optimal separating hyperplane can be represented by a decision function, which is learned from the training set to predict the class label in the subsequent tests. In order to formulate the SVM algorithm based on radial basis function, suppose that a training set consists of N samples and couple (x_i, y_i) describes data element $\{x_i, i = 1, 2, \ldots, N\}$ and the corresponding class label y_i. The decision function can be formulated as (8), (9):

$$Y = \sum_{i\in \mathrm{SVs}} w_i K(x, x_i) + b \tag{8}$$

$$K(x, x_i) = \exp\left(-\gamma \|x - x_i\|^2\right), \tag{9}$$

where w is support vector coefficient, which is the product of the Lagrange multiplier, b is the bias term, and $K(x, x_i)$ is the kernel function (RBF function is adopted in this work) which can solve the problem of linear indivisibility in primitive space by mapping data to high dimension space. SVs represents support vectors, namely, the training data examples.

For the implementation of SVM classifier, a library of SVM, LIBSVM [53] is used. The performance of SVM classifier depends on choice of two parameters: error penalty factor C and kernel function parameter γ. In this study, grid search approach is employed to find the optimal values of C and γ. The parameters C and γ were set as 32 and 0.01956 respectively, with which the highest cross validation accuracy was achieved.

3) K-NEAREST NEIGHBOR

The KNN algorithm is an instance-based supervised method which is based on feature similarity: how closely out-of-sample features resemble the training set determines how the given data is classified [54]. The distance between two instances $\boldsymbol{x}_i$ and $\boldsymbol{x}_j$ can be measured in different forms, for example, Euclidean Distance (ED), City Block distance, Minkowski Distance (MID), as shown in (10), (11), and (12), respectively:

$$f\left(\boldsymbol{x}_i, \boldsymbol{x}_j\right) = \left(\sum_{k=1}^{p}\left(\boldsymbol{x}_i(k) - \boldsymbol{x}_j(k)\right)^2\right)^{1/2} \tag{10}$$

$$f\left(\boldsymbol{x}_i, \boldsymbol{x}_j\right) = \frac{1}{p}\sum_{k=1}^{p}\left|\boldsymbol{x}_i(k) - \boldsymbol{x}_j(k)\right| \tag{11}$$

$$f\left(\boldsymbol{x}_i, \boldsymbol{x}_j\right) = \left(\sum_{k=1}^{p}\left(\boldsymbol{x}_i(k) - \boldsymbol{x}_j(k)\right)^r\right)^{1/r} \tag{12}$$

where $f(\boldsymbol{x}_i, \boldsymbol{x}_j)$ is the distance function and p is the dimension of the feature vector space. The test instance $\boldsymbol{x}_i$ belongs to the nearest the class with the major votes of its K-nearest neighbors. In this work, Euclidean distance was used as the measure function. The value of K was altered from 20 to 35, and the optimal K was concluded to be 31 for which the best accuracy for the test samples was obtained.

III. EXPERIMENTAL RESULT

In this section, we will describe the ECG database, evaluation metrics used to evaluate our proposed system, and present our results.

A. ECG DATA DESCRIPTION

In order to validate the effectiveness of the proposed ECG arrhythmia recognition and classification system, realistic ECG data from MIT-BIH arrhythmia database [49] were adopted. The MIT-BIH arrhythmia database includes 48 ECG recordings at a sampling frequency of 360 Hz with 11-bit of resolution over a 10 mV range. There are two channels of data, lead A, a modified limb lead II (MLII) and lead B, a modified lead V1 (occasionally V2 or V5, and in one instance V4). An ECG signal example with Lead MLII and Lead V5 from the MIT-BIH arrhythmia database is shown in Fig. 4. Since lead MLII highlights the most important waves within the heartbeat, such as P wave and QRS complex, which correspond to the atrial depolarization and ventral depolarization respectively, it is one of the most utilized lead for diagnosing heart diseases and was also adopted in our work. Recording 102 and 104 that have no lead II information were excluded. Hence, a total of 46 records, which lead A is lead MLII or lead B is lead MLII (recording 114) were used for classification of heartbeats from MIT-BIH arrhythmia database in this study. Each recording contains an annotation.atr file where each heartbeat is labeled with its type. These labels are used to evaluate the accuracy of the classification. According to the ANSI/AAMI EC57:1998/(R) 2008 standard [55], the original 15 heartbeat types from the MIT-BIH arrhythmia data are grouped into several superclasses: normal (N), supraventricular ectopic beat (SVEB), ventricular ectopic beat (VEB), fusion beat (F), and unknown beat (Q). Table 1 illustrates the corresponding

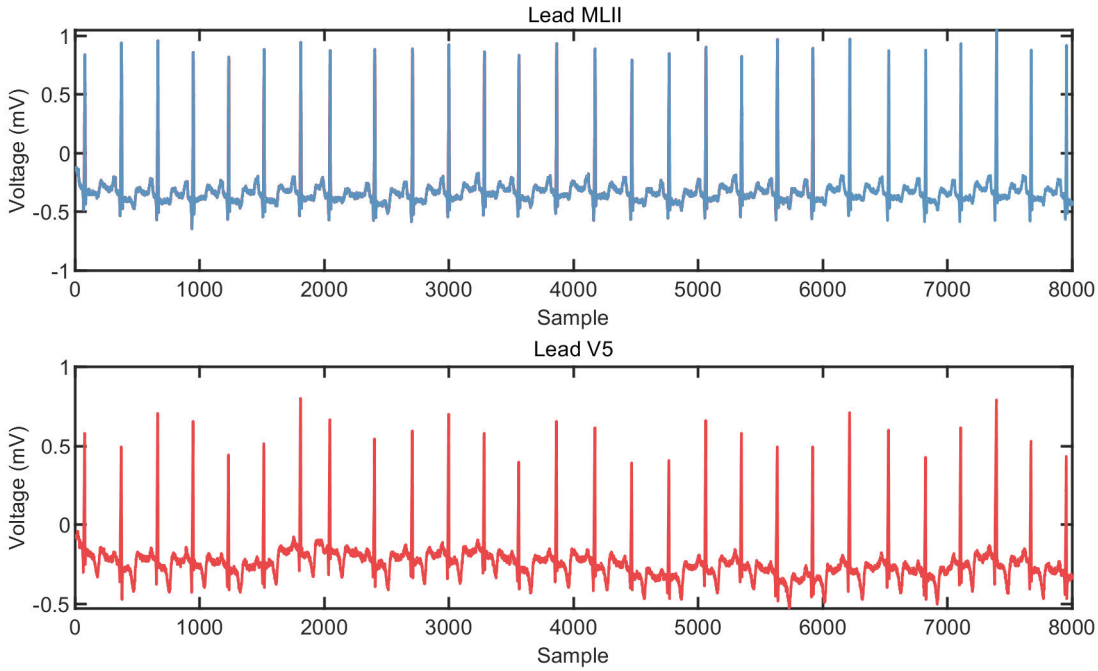

FIGURE 4. The ECG signal example with Lead MLII and Lead V5 from the MIT-BIH arrhythmia database.

relationship between heartbeat types in the MIT-BIH arrhythmia database and those in the AAMI standard. All 15 types of heartbeat were adopted in this study. However, the heartbeats without complete cycle were discarded due to lack of inter-beat features. The final data size of this study is given in Table 1. All the experiments were performed using Matlab R2018b programming environment on a desktop PC with Intel(R) Core i5-7500 CPU (3.30 GHz) and 32 GB RAM configuration.

B. EVALUATION METRICS

To evaluate the performance of the proposed system, the ten-fold cross-validation technique was used for training and testing the classifier. And then, three standard statistical metrics, F_1 score, precision (also referred to as positive predictivity P+), and accuracy (Acc) were derived from four parameters: numbers of true-positives (TP), true-negatives (TN), false-negatives (FN) and false-positives (FP) respectively as (13), (14), and (15):

$$\mathrm{F_1\ score} = \frac{\mathrm{Precision} \times \mathrm{Recall}}{(\mathrm{Precision} + \mathrm{Recall})} \times 2 \tag{13}$$

$$\mathrm{Precision} = \frac{\mathrm{TP}}{(\mathrm{TP} + \mathrm{FP})} \tag{14}$$

$$\mathrm{Acc} = \frac{\mathrm{TP} + \mathrm{TN}}{(\mathrm{TP} + \mathrm{FP} + \mathrm{TN} + \mathrm{FN})} \tag{15}$$

where Recall refers to the ratio of true positives to the all observations in actual classčTrue, as defined in (16):

$$\mathrm{Recall} = \frac{\mathrm{TP}}{(\mathrm{TP} + \mathrm{FN})} \tag{16}$$

C. RESULTS

The proposed clustering-based feature extraction algorithm has been applied to extract and classify visual morphological pattern of QRS complex. According to Section II. B. 2), there are two parameters T_c and $\mathrm{C_{max}}$ that should be tuned properly to attain satisfactory results. Considering there were 15 types of heartbeats involved in this work and the ECG waveform similarity of the same arrhythmia type, the $C_{\max}$ was set to 15. It should be noted that more clusters can be created when conditions are met according to Algorithm 1. On the other hand, since normal heartbeat is the main type among all the heartbeat types, one reasonable solution to find the proper threshold (T_c) is to reduce the number of abnormal heartbeats clustered as normal type to a minimum. In this study, the proper choice for T_c was concluded to be 0.78. The results of application of the proposed AKMC feature extraction algorithm are shown in Fig. 5, where a total of 21 VMP-QRSs were obtained.

In the proposed arrhythmia recognition and classification system, the extracted features, i.e., parameters and extracted VMP-QRSs, were fed into three classifiers. In order to compare the increase of discriminating power of the proposed features, the extracted features were divided into two feature sets, namely, the classical parametric features (feature set1) and the proposed VMP-QRS feature (feature set2). Table 2 illustrates the accuracies obtained with different feature sets and classifiers. To better compare the classification results in terms of various heartbeat types though different feature sets, we visualize the classification accuracy of each heartbeat type in form of the bar chart in Fig. 6, which clearly shows that the proposed combined feature set1 and

TABLE 1. The corresponding relationship between AAMI standard and heartbeat types in the MIT-BIH arrhythmia database as well as the summary of the data size adopted in this study.

AAMI Class	MIT-BIH Annotation	Type	Total # of Heartbeats
Normal (N)	N	Normal beat	74722
	L	Left bundle branch block beat	8069
	R	Right bundle branch block beat	7250
	e	Atrial escape beat	16
	j	Nodal escape	229
Supraventricular ectopic beat (SVEB)	A	Atrial premature beat	2544
	a	Aberrated atrial premature beat	150
	J	Nodal (junctional) premature beat	83
	S	Supraventricular premature beat	2
Ventricular ectopic beat (VEB)	V	Premature ventricular contraction	7122
	E	Ventricular escape beat	106
Fusion beat (F)	F	Fusion of ventricular and normal beat	802
Unknown beat (Q)	P or /	Paced beat	3616
	f	Fusion of paced and normal beat	260
	Q	Unclassifiable beat	15
		Total # of Heartbeats	104986

set2 yielded much more accurate classification accuracy compared to the classical feature set1 in this arrhythmia classification scenario.

To further research on the performance of the proposed method with KNN classifier, we summarize the statistical information, i.e., F_1 score and precision, in Table 3.

IV. DISCUSSION

This paper provides an arrhythmia recognition and classification method using combined parametric and a novel visual pattern feature of ECG morphology. Generally, the effectiveness of the proposed method and the novel morphological feature is justified by the experimental results shown in Section III. The performance of our proposed method from different perspectives are discussed in details as following.

A. A STUDY ON THE VISUAL MORPHOLOGICAL PATTERN OF QRS COMPLEX

As can be seen in Fig. 4, all the QRS complex morphology vectors representing 15 types of heartbeat were automatically classified into 21 patterns based on shape similarity. This result reveals the fact that in most cases, the same heartbeat type exhibits a similar morphology, but it is not always the case. It also demonstrates that the actual created number of visual morphological patterns of QRS complex using our proposed feature extraction AKMC algorithm could adapt to the input QRS complex vectors. Among all the patterns, pattern (a) contained the largest number of the vectors, with the waveform of centroid similar to the normal beats. Some patterns are similar, for example, pattern (j) and (l). However, they are still distinguishable through distance comparison. Pattern (d), (e), (g), (m), (n), (o), (q), (r), (t) and (u) indicate a large difference in QRS complex morphology, which reflects different atrial or ventral conduction defects. Some abnormal QRS morphologies with very limited number of heartbeats were shown in the rest patterns. For example, two clearly different QRS complex morphologies appeared in pattern (f) and (h). According to the annotation file from MIT-BIT arrhythmia database, these two QRS complex morphologies correspond to premature ventricular contraction (V) beats. Though the extracted VMP-QRS feature, these different QRS complex morphologies could be easily distinguished from each other in shape and visualized as medical

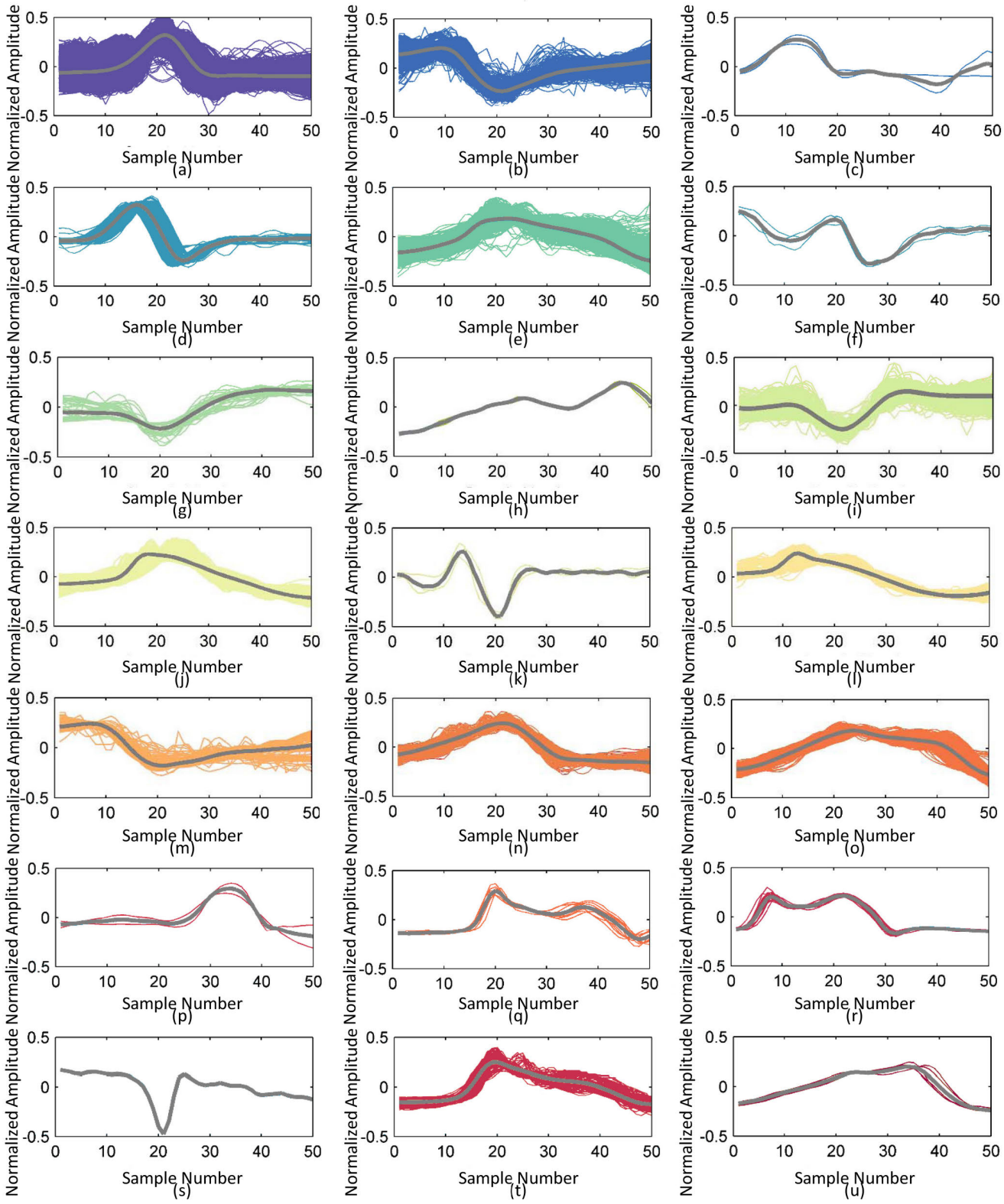

FIGURE 5. Extracted visual morphological patterns of QRS complex for heartbeats from the MIT-BIH arrhythmia database. Gray line represents the centroid of each pattern; while lines in other colors represent original QRS complex segments assigned to the corresponding patterns.

predictors of certain types of arrhythmias for a medium or long term ECG diagnosis. This fact implies that our proposed method is able to extract the hidden information from the ECG signal. In addition, it can substantially ease the burden of manually inspection of the long-term ECG records.

TABLE 2. A summary of the accuracy achieved using combinations of feature sets and different classifiers (NN, SVM, and KNN) in the assessment.

Types	NN		SVM		KNN	
	Feature Set1 Acc(%)	Feature Set1 & Set2 Acc(%)	Feature Set1 Acc(%)	Feature Set1 & Set2 Acc(%)	Feature Set1 Acc(%)	Feature Set1 & Set2 Acc(%)
N	85.97	96.65	85.94	94.53	86.64	97.79
L	75.99	94.61	86.43	95.39	78.68	99.50
R	82.62	99.33	85.23	99.09	95.03	99.59
e	50.00	50.00	50.00	50.00	50.00	50.00
j	51.74	53.93	50.44	51.09	60.89	70.28
A	54.84	84.98	58.36	81.71	59.68	89.70
a	54.27	59.33	51.00	53.33	50.66	77.99
J	50.50	51.01	50.60	51.20	52.40	67.46
S	50.00	50.00	50.00	50.00	50.00	50.00
V	92.20	96.98	82.53	94.82	92.34	97.69
E	72.39	93.86	83.02	96.22	51.88	92.45
F	69.28	76.77	53.74	57.41	54.46	87.19
P	97.46	99.83	97.12	99.71	95.89	99.92
f	62.87	68.26	55.96	60.77	85.76	95.38
Q	50.00	50.00	50.00	50.00	50.00	50.00
Overall Accuracy	84.68	96.11	84.93	94.23	86.23	**97.70**

Therefore, the proposed VMP-QRS feature along with the AKMC algorithm is further verified to be suitable as a new methodology to extract QRS complex morphology information which can be used in arrhythmia recognition and classification while allowing the doctors to comprehend intuitively. What's more, the proposed AKMC algorithm has minimal number of parameters, i.e. two parameters, to be adjusted, which implies that the proposed methods are possible to be conveniently and universally applied in the clinic or mobile devices.

B. PERFORMANCE OF THE PROPOSED ARRHYTHMIA RECOGINITION AND CLASSIFICATION SYSTEM

It can be seen from Table 2 that all classifiers achieved a notably better overall accuracy utilizing the combined feature set1 and the proposed feature VMP-QRS than that of solely feature set1 based method, with an increase of 11.43%, 9.30%, and 11.47% for NN, SVM, and KNN, respectively. The best result with respect to overall accuracy was 97.70% achieved using KNN and combination of features set1 and set2, followed by NN (96.11%) and SVM (94.23%). Hence, the effectiveness of our proposed method is generally validated.

Besides, Fig. 6 indicates that the advantage in accuracy using the proposed features does continue uniformly for all types, especially for six main types of heartbeats, i.e. N, L, R, A, V and P, which compose around 98.41% of all instances. The increases in classification accuracy utilizing KNN and combination of feature set1 and set 2 for the type of N, L, R, A, V, and P were 11.15%, 20.82%, 4.56%, 30.02%, 5.35%, and 4.03%, respectively.

From evaluation in terms of the statistical indicators, as shown in Table 3, the F_1 score and precision have obvious improvements for most of the heartbeat types in this study. One explanation for this is that different electrical activity during ventricular depolarization can be reflected on QRS complex morphology changes. It is an essential step for medical practitioners to infer various types of cardiac dysfunctions through a fine visual analysis of the irregular changes in ECG waveforms. These fundamental intuitions used by physicians are employed in our proposed new feature, i.e. VMP-QRS, and consequently contribute

TABLE 3. A summary of statistical indicators using combinations of feature sets and KNN classifier in the assessment. The metrics are: F_1 score (F_1) and precision (P+).

KNN	(%)	N	L	R	e	j	A	a	J	S	V	E	F	P	f	Q
Feature Set1	F_1	87.76	73.44	94.84	-	35.82	32.99	2.63	9.19	-	91.8	7.27	16.66	95.72	83.39	-
	P+	80.99	97.39	98.47	-	99.73	97.55	99.01	99.74	-	98.76	99.77	98.01	99.82	99.96	0
Feature Set1 & Set2	F_1	97.82	99.5	99.59	-	57.74	88.56	71.79	51.78	-	97.64	91.83	85.34	99.92	95.16	-
	P+	96.74	99.87	99.86	0	99.88	99.61	99.96	99.94	0	99.6	100	99.76	99.99	99.99	0

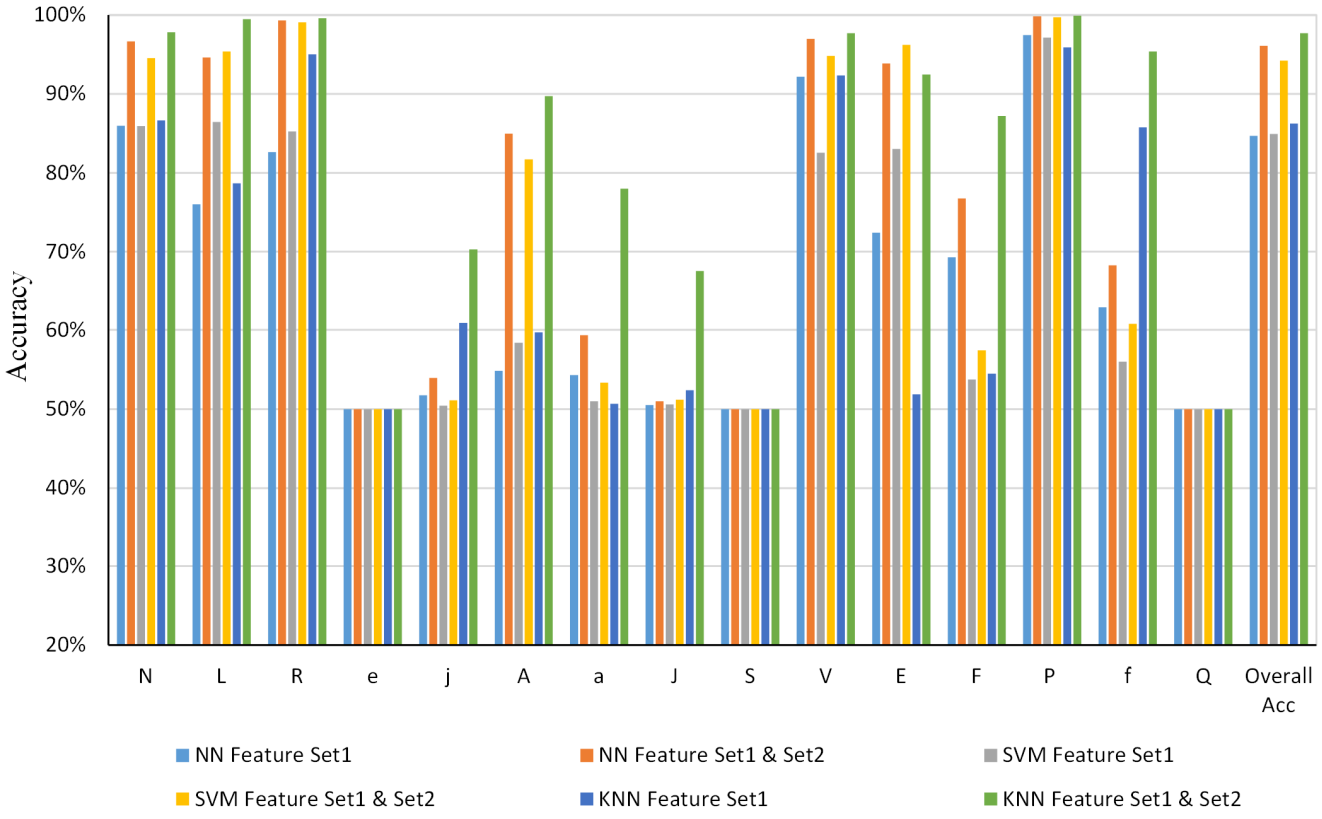

FIGURE 6. Comparison of accuracy achieved using combinations of feature sets and different classifiers (NN, SVM, and KNN) in terms of heartbeat type and overall accuracy.

to the accurate arrhythmia discrimination in the experiment. Although parametric features (feature set1) are good at spotting major disease differences, these features cannot explicitly model the morphological changes in details. In this study, abnormal heartbeats with parametric features in normal range can be easily distinguished from normal heartbeats using the proposed visual morphological pattern feature. As a result, the proposed method obtained a remarkable performance improvement for most heartbeat types, for example, type N, with a F_1 score increase of 10.06% and a precision increase of 15.75%. Hence, the reliability and accuracy of the proposed method is further verified.

However, all feature sets report limited results with type e, S, and Q, since the MIT-BIH arrhythmia database contains only 2 instances of S, 16 instances of e, and 15 instances of Q, which are quite insufficient for a reliable learning. Thus, the classification methods do not have the possibility to correctly recognize heartbeats.

C. A COMPARISON WITH RECENT APPROACHES

Moreover, in order to validate the performance improvement of the proposed method for ECG arrhythmia classification, a comparison with other relevant high-performance works was performed. The result of comparison is presented in Table 4.

TABLE 4. Comparison of the classification performance of the proposed method with recent approaches.

Authors	Year	Feature	Classifier	Type	Data Size	Accuracy
Ye et al. [56]	2012	DWT+ICA+PCA	SVM-RBF	5	100688	94.00%
Zhang et al. [29]	2014	ECG Morphology	SVM-RBF	4	101398	86.66%
Pławiak et al. [36]	2018	Frequency components of the PSD	Evolutionary Neural System (based on single SVM)	15	1000 (segments)	91.00%
Venkatesan et al. [25]	2018	HRV Parameters	SVM	2	N/A	96.00%
Oh et al. [43]	2018	Normalized ECG Data	CNN+LSTM	5	16499 (segments)	98.10%
Marinho et al. [11]	2019	SCM+Fourier+HOS+Goertzel	Bayes	5	100467	94.30%
Yang et al. [42]	2019	Raw Data	DL-CCANeT	15	3350	95.25%
Pławiak et al. [45]	2019	Frequency components of the PSD	Deep Genetic Ensemble of Classifiers	17	744 (segments)	95.00%
This study	2020	Parameter +Visual Pattern of ECG Morphology	KNN	15	104986	97.70%

In [56], Ye *et al.* achieved an accuracy of 94.00% for classifying a total number of 100688 heartbeats into five categories using DWT coefficients with PCA and ICA. In other literature, ECG morphological features, such as amplitude, area, etc. were employed for four classes of beats and obtained an overall accuracy of 86.66% [29]. Plawiak used the PSD estimated based on Welch's method and discrete Fourier transform as ECG signal features to train a SVM-based evolutionary-neural system and a 3-layer deep genetic ensemble of classifiers (DGEC), then achieved an overall accuracy of 91.00% [36] and 95.00% [45], respectively. Oh *et al.* [43] proposed an automated diagnosis system using a combination of CNN and long short-term memory (LSTM) for diagnosis of N, L, R, A, and V, achieving an accuracy of 98.10% when validated with 16499 segments from MIT-BIH arrhythmia database. Venkatesan *et al.* [25] applied DWT for HRV feature extraction and classified ECG signal into normal and abnormal classes using SVM classifier with a maximum accuracy of 96.00%.

As Table 4 shows, it is different both in the data size and number of heartbeat types, which are two items to note for a fair comparison. First, the evaluation data size could affect the validity of the methods. In our work, all the patients' records (excluded two records due to lack of signal from Lead II) with a total of 104986 heartbeats from MIT-BIH arrhythmia database were adopted in our assessment to ensure the validity. Second, we desire to aid medical diagnosis by classifying all the heartbeat types categorized by ANSI/AAMI EC57:1998/(R) 2008 standard. The evaluation of this work was based on these two perspectives, which means it is more realistic and reliable in real case scenario because patients and types vary in clinical practice. The comparison results shown in Table 4 indicate that our proposed method, taking into account the data size and the number of heartbeat types classified, achieved a higher performance than the other studies dealing with arrhythmia classification. The comparison results verify that our proposed method can serve as an effective and reliable tool for cardiologists in this ECG arrhythmia diagnosis case. In addition, it has the advantages of lower computational cost and fewer parameters to set up, which implies that the proposed method could be an efficient medical aid system to diagnose heart disease.

V. CONCLUSION

ECG is an important non-invasively tool widely used in cardiovascular disease diagnosis. Abnormal heart electrical activity can cause irregular morphology changes in ECG signals, through which the medical practitioners can detect various types of cardiac arrhythmia.

In this paper, we propose an effective arrhythmia recognition and classification system consisting of preprocessing and detection, feature extraction, and heartbeat classification.

Considering the performance of arrhythmia recognition and classification system has strong dependence on the feature extraction, a novel discriminating feature, VMP-QRS, as well as a new feature extraction algorithm, AKMC, is introduced in our work. The key idea that patients with similar type of arrhythmia have similarities in their ECG waveforms and the fact that physicians routinely perform inference and diagnosis with visual examination of ECG waveform morphology, are utilized in the proposed feature, i.e., VMP-QRS, and implemented into the computational AKMC algorithm for extracting this feature. The performance of the proposed method is evaluated with all 15 different heartbeat types categorized by ANSI/AAMI EC57:1998/(R) 2008 standard from MIT-BIT arrhythmia database and achieves the best overall accuracy of 97.70% and the accuracies of 97.79%, 99.50%, 99.59%, 97.69%, 89.70%, and 99.92% for the six main heartbeat types N, L, R, V, A, and P respectively, utilizing KNN classifier and combined feature sets. Comparison of classification performance of the proposed method with some high-performance methods also justified a better performance in automatic cardiac arrhythmia classification technologies.

Due to the promising results obtained, there is potential to use our solution in telemedicine and implement designed method in mobile devices or cloud computing with the advantage of lower computational complexity, low cost and few parameters to configure. Since the extracted VMP-QRS is based on the physiological meaning, it allows medical practitioners to better understand and use the result as a medical predictor of certain pathologies as well.

The limitation of this study is that we mainly focus on the visual patterns of the main wave in ECG signal, i.e., the QRS complex. In the future, the variability of other ECG waves, such us P waves, and T waves should be studied based on the proposed feature extraction algorithm to further improve the performance of the whole system.

REFERENCES

[1] S. Mendis, S. Davis, and B. Norrving, "Organizational update: The world health organization global status report on noncommunicable diseases 2014; one more landmark step in the combat against stroke and vascular disease," *Stroke*, vol. 46, no. 5, pp. e121–e122, May 2015.

[2] B. Hemmeryckx, Y. Feng, L. Frederix, M. Lox, S. Trenson, R. Vreeken, H. R. Lu, D. Gallacher, Y. Ni, and H. R. Lijnen, "Evaluation of cardiac arrhythmic risks using a rabbit model of left ventricular systolic dysfunction," *Eur. J. Pharmacol.*, vol. 832, pp. 145–155, Aug. 2018.

[3] P. E. McSharry, G. D. Clifford, L. Tarassenko, and L. A. Smith, "A dynamical model for generating synthetic electrocardiogram signals," *IEEE Trans. Biomed. Eng.*, vol. 50, no. 3, pp. 289–294, Mar. 2003.

[4] S. H. Jambukia, V. K. Dabhi, and H. B. Prajapati, "Classification of ECG signals using machine learning techniques: A survey," in *Proc. Int. Conf. Adv. Comput. Eng. Appl. (ICACEA)*, Ghaziabad, India, Mar. 2015, pp. 714–721.

[5] A. Gotchev, N. Nikolaev, and K. Egiazarian, "Improving the transform domain ECG denoising performance by applying inter-beat and intra-beat decorrelating transforms," in *Proc. IEEE Int. Symp. Circuits Syst. (ISCAS)*, Sydney, NSW, Australia, May 2001, pp. 17–20.

[6] L. Wang, W. Sun, Y. Chen, P. Li, and L. Zhao, "Wavelet transform based ECG denoising using adaptive thresholding," in *Proc. 7th Int. Conf. Bioinf. Biomed. Sci. (ICBBS)*, Shenzhen, China, Jun. 2018, pp. 35–40.

[7] W.-H. Jung and S.-G. Lee, "ECG identification based on non-fiducial feature extraction using window removal method," *Appl. Sci.*, vol. 7, no. 11, Nov. 2017, Art. no. 1205, doi: 10.3390/app7111205.

[8] S. Poungponsri and X.-H. Yu, "An adaptive filtering approach for electrocardiogram (ECG) signal noise reduction using neural networks," *Neurocomputing*, vol. 117, no. 87, pp. 206–213, Oct. 2013.

[9] M. Rakshit and S. Das, "An efficient ECG denoising methodology using empirical mode decomposition and adaptive switching mean filter," *Biomed. Signal Process. Control*, vol. 40, pp. 140–148, Feb. 2018.

[10] T. He, G. Clifford, and L. Tarassenko, "Application of independent component analysis in removing artefacts from the electrocardiogram," *Neural Comput. Appl.*, vol. 15, no. 2, pp. 105–116, Apr. 2006.

[11] L. B. Marinho, N. D. M. M. Nascimento, J. W. M. Souza, M. V. Gurgel, P. P. R. Filho, and V. H. C. de Albuquerque, "A novel electrocardiogram feature extraction approach for cardiac arrhythmia classification," *Future Gener. Comput. Syst.*, vol. 97, pp. 564–577, Aug. 2019.

[12] A. F. Khalaf, M. I. Owis, and I. A. Yassine, "A novel technique for cardiac arrhythmia classification using spectral correlation and support vector machines," *Expert Syst. Appl.*, vol. 42, no. 21, pp. 8361–8368, Nov. 2015.

[13] M. Thomas, M. K. Das, and S. Ari, "Automatic ECG arrhythmia classification using dual tree complex wavelet based features," *AEU-Int. J. Electron. Commun.*, vol. 69, no. 4, pp. 715–721, Apr. 2015.

[14] M. A. Escalona-Morán, M. C. Soriano, I. Fischer, and C. R. Mirasso, "Electrocardiogram classification using reservoir computing with logistic regression," *IEEE J. Biomed. Health Informat.*, vol. 19, no. 3, pp. 892–898, May 2015.

[15] I. Christov, V. Krasteva, I. Simova, T. Neycheva, and R. Schmid, "Multiparametric analysis for atrial fibrillation classification in the ECG," in *Proc. Comput. Cardiol. Conf. (CinC)*, Rennes, France, Sep. 2017, pp. 1–4.

[16] N. Razmjooy, M. Ramezani, and N. Ghadimi, "Imperialist competitive algorithm-based optimization of neuro-fuzzy system parameters for automatic red-eye removal," *Int. J. Fuzzy Syst.*, vol. 19, no. 4, pp. 1144–1156, Aug. 2017, doi: 10.1007/s40815-017-0305-2.

[17] Y. Kaya and H. Pehlivan, "Classification of premature ventricular contraction in ECG," *Int. J. Adv. Comput. Sci. Appl.*, vol. 6, no. 7, pp. 34–40, Jul. 2015.

[18] Y. Kaya, H. Pehlivan, and M. E. Tenekeci, "Effective ECG beat classification using higher order statistic features and genetic feature selection," *Biomed. Res.*, vol. 28, no. 17, pp. 7594–7603, Aug. 2017.

[19] Y. Özbay and G. Tezel, "A new method for classification of ECG arrhythmias using neural network with adaptive activation function," *Digit. Signal Process.*, vol. 20, no. 4, pp. 1040–1049, Jul. 2010.

[20] P. De Chazal, M. O'Dwyer, and R. B. Reilly, "Automatic classification of heartbeats using ECG morphology and heartbeat interval features," *IEEE Trans. Biomed. Eng.*, vol. 51, no. 7, pp. 1196–1206, Jul. 2004.

[21] C.-C. Lin and C.-M. Yang, "Heartbeat classification using normalized RR intervals and morphological features," *Math. Problems Eng.*, vol. 2014, May 2014, Art. no. 712474.

[22] M. Llamedo and J. P. Martínez, "Heartbeat classification using feature selection driven by database generalization criteria," *IEEE Trans. Biomed. Eng.*, vol. 58, no. 3, pp. 616–625, Mar. 2011.

[23] M. G. Tsipouras and D. I. Fotiadis, "Automatic arrhythmia detection based on time and time–frequency analysis of heart rate variability," *Comput. Methods Programs Biomed.*, vol. 74, no. 2, pp. 95–108, May 2004.

[24] U. R. Acharya, P. S. Bhat, S. S. Iyengar, A. Rao, and S. Dua, "Classification of heart rate data using artificial neural network and fuzzy equivalence relation," *Pattern Recognit.*, vol. 36, no. 1, pp. 61–68, Jan. 2003.

[25] C. Venkatesan, P. Karthigaikumar, A. Paul, S. Satheeskumaran, and R. Kumar, "ECG signal preprocessing and SVM classifier-based abnormality detection in remote healthcare applications," *IEEE Access*, vol. 6, pp. 9767–9773, 2018.

[26] I. Jekova, G. Bortolan, and I. Christov, "Assessment and comparison of different methods for heartbeat classification," *Med. Eng. Phys.*, vol. 30, no. 2, pp. 248–257, Mar. 2008.

[27] M. Korürek and B. Doğan, "ECG beat classification using particle swarm optimization and radial basis function neural network," *Expert Syst. Appl.*, vol. 37, no. 12, pp. 7563–7569, Dec. 2010.

[28] R. G. Afkhami, G. Azarnia, and M. A. Tinati, "Cardiac arrhythmia classification using statistical and mixture modeling features of ECG signals," *Pattern Recognit. Lett.*, vol. 70, pp. 45–51, Jan. 2016.

[29] Z. Zhang, J. Dong, X. Luo, K.-S. Choi, and X. Wu, "Heartbeat classification using disease-specific feature selection," *Comput. Biol. Med.*, vol. 46, no. 1, pp. 79–89, Mar. 2014.

[30] C. Lin, Y. Du, and T. Chen, "Adaptive wavelet network for multiple cardiac arrhythmias recognition," *Expert Syst. Appl.*, vol. 34, no. 4, pp. 2601–2611, May 2008.

[31] Y. Kutlu and D. Kuntalp, "Feature extraction for ECG heartbeats using higher order statistics of WPD coefficients," *Comput. Methods Programs Biomed.*, vol. 105, no. 3, pp. 257–267, Mar. 2012.
[32] T. Tuncer, S. Dogan, P. Pławiak, and U. R. Acharya, "Automated arrhythmia detection using novel hexadecimal local pattern and multilevel wavelet transform with ECG signals," *Knowl.-Based Syst.*, vol. 186, Dec. 2019, Art. no. 104923, doi: 10.1016/j.knosys.2019.104923.
[33] I. Guler and E. Ubeyli, "ECG beat classifier designed by combined neural network model," *Pattern Recognit.*, vol. 38, no. 2, pp. 199–208, Feb. 2005.
[34] S.-N. Yu and Y.-H. Chen, "Electrocardiogram beat classification based on wavelet transformation and probabilistic neural network," *Pattern Recognit. Lett.*, vol. 28, no. 10, pp. 1142–1150, Jul. 2007.
[35] S. Kara and M. Okandan, "Atrial fibrillation classification with artificial neural networks," *Pattern Recognit.*, vol. 40, no. 11, pp. 2967–2973, Nov. 2007.
[36] P. Pławiak, "Novel methodology of cardiac health recognition based on ECG signals and evolutionary-neural system," *Expert Syst. Appl.*, vol. 92, pp. 334–349, Feb. 2018.
[37] R. J. Martis, U. R. Acharya, K. M. Mandana, A. K. Ray, and C. Chakraborty, "Cardiac decision making using higher order spectra," *Biomed. Signal Process. Control*, vol. 8, no. 2, pp. 193–203, Mar. 2013.
[38] C. Ye, M. T. Coimbra, and B. V. Kumar, "Arrhythmia detection and classification using morphological and dynamic features of ECG signals," in *Proc. IEEE Ann. Int. Conf. Eng. Med. Biol. Soc. (EMBC)*, Buenos Aires, Argentina, Aug. 2010, pp. 1918–1921.
[39] M. P. S. Chawla, "A comparative analysis of principal component and independent component techniques for electrocardiograms," *Neural Comput. Appl.*, vol. 18, no. 6, pp. 539–556, Sep. 2009.
[40] R. J. Martis, U. R. Acharya, and L. C. Min, "ECG beat classification using PCA, LDA, ICA and discrete wavelet transform," *Biomed. Signal Process. Control*, vol. 8, no. 5, pp. 437–448, Sep. 2013.
[41] C. Amuthadevi, "Effective ECG beat classification using colliding bodies," *Biomed. Res.*, vol. 28, pp. 307–314, Mar. 2017.
[42] W. Yang, Y. Si, D. Wang, and G. Zhang, "A novel approach for multi-lead ECG classification using DL-CCANet and TL-CCANet," *Sensors*, vol. 19, no. 14, Jul. 2019, Art. no. 3214.
[43] S. L. Oh, E. Y. K. Ng, R. S. Tan, and U. R. Acharya, "Automated diagnosis of arrhythmia using combination of CNN and LSTM techniques with variable length heart beats," *Comput. Biol. Med.*, vol. 102, pp. 278–287, Nov. 2018.
[44] L. Qian, J. Wang, L. Jin, Y. Huang, J. Zhang, H. Zhu, S. Yan, and X. Wu, "Optimized convulutional neural network by genetic alorithm for the classification of complex arrhythmia," *J. Med. Imag. Health Inform.*, vol. 9, no. 9, pp. 1905–1912, Dec. 2019.
[45] P. Pławiak and U. R. Acharya, "Novel deep genetic ensemble of classifiers for arrhythmia detection using ECG signals," in *Neural Computing and Applications*. Springer, Jan. 2019, pp. 1–25, doi: 10.1007/s00521-018-03980-2.
[46] C.-H. Lin, "Frequency-domain features for ECG beat discrimination using grey relational analysis-based classifier," *Comput. Math. Appl.*, vol. 55, no. 4, pp. 680–690, Feb. 2008.
[47] J. Pan and W. J. Tompkins, "A real-time QRS detection algorithm," *IEEE Trans. Biomed. Eng.*, vol. BME-32, no. 3, pp. 230–236, Mar. 1985.
[48] E. J. D. S. Luz, W. R. Schwartz, G. Cámara-Chávez, and D. Menotti, "ECG-based heartbeat classification for arrhythmia detection: A survey," *Comput. Methods Programs Biomed.*, vol. 127, pp. 144–164, Apr. 2016.
[49] A. L. Goldberger, L. A. N. Amaral, L. Glass, J. M. Hausdorff, P. C. Ivanov, R. G. Mark, J. E. Mietus, G. B. Moody, C.-K. Peng, and H. E. Stanley, "PhysioBank, PhysioToolkit, and PhysioNet: Components of a new research resource for complex physiologic signals," *Circulation*, vol. 101, no. 23, pp. e215–e220, Jun. 2000.
[50] R. O. Duda, P. E. Hart, and D. G. Stork, "Unsupervised learning and clustering," in *Pattern Classification*, 2nd ed. New York, NY, USA: Wiley, 2001, pp. 526–528.
[51] J. Schmidhuber, "Deep learning in neural networks: An overview," *Neural Netw.*, vol. 61, pp. 85–117, Jan. 2015.
[52] C. M. Bishop, *Pattern Recognition and Machine Learning*. Berlin, Germany: Springer, 2007, pp. 236–240.
[53] C. C. Chang and C. J. Lin, "LIBSVM: A library for support vector machines," *ACM Trans. Intell. Syst. Technol.*, vol. 2, no. 3, Apr. 2011, Art. no. 27.
[54] N. Bhatia, "Survey of nearest neighbor techniques," *Int. J. Comput. Sci. Inf. Secur.*, vol. 8, no. 2, pp. 302–305, Jan. 2010.
[55] *ANSI/AAMI, Testing and reporting performance results of cardiac rhythm and ST segment measurement algorithms*, Standard ANSI/AAMI/ISO EC57, 1998-(R)2008, American National Standards Institute, Association for the Advancement of Medical Instrumentation, 2008.
[56] C. Ye, B. V. Kumar, and M. T. Coimbra, "Combining general multi-class and specific two-class classifiers for improved customized ECG heartbeat classification," in *Proc. 21st Int. Conf. Pattern Recognit. (ICPR)*, Tsukuba, Japan, Nov. 2012, pp. 2428–2431.

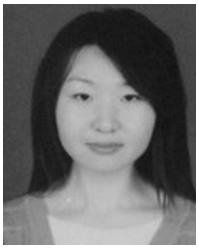

HUI YANG (Member, IEEE) received the B.Eng. degree in applied electronics technology from Qingdao Ocean University (Ocean University of China), Qingdao, China, in 2002, and the M.Sc. degree in advanced photonics and communications from the University of Warwick, Coventry, U.K., in 2005. She is pursuing the Ph.D. degree with the College of Information Science and Engineering, Ocean University of China. Since 2006, she has been working with the Department of Computer Foundation, Ocean University of China, where she is currently a Lecturer. Her areas of interests include signal processing, machine learning, and intelligent computing.

ZHIQIANG WEI received the B.Eng. degree from Shandong University, Jinan, China, in 1992, the M.Sc. degree from the Harbin Institute of Technology, Harbin, China, in 1995, and the Ph.D. degree from Tsinghua University, Beijing, China, in 2001. He is currently a Professor with the Ocean University of China. His main research interests include signal processing, software engineering, and intelligent computing.